Manipulating the Dynamics of Self-Propelled Gallium Droplets by Gold Nanoparticles and Nanoscale Surface Morphology

Alexei A. Zakharov,[‡] Erik Mårsell,[†] Emelie Hilner,[†] Rainer Timm,[†] Jesper N. Andersen,[‡] Edvin Lundgren,[†] and Anders Mikkelsen*[,†]

[†]Department of Physics and the Nanometer Structure Consortium (nmC@LU) and [‡]MAX IV Laboratory, Lund University, P.O. Box 118, 221 00 Lund, Sweden

ABSTRACT Using *in situ* surface-sensitive electron microscopy performed in real time, we show that the dynamics of micron-sized Ga droplets on GaP(111) can be manipulated locally using Au nanoparticles. Detailed measurements of structure and dynamics of the surface from microns to atomic scale are done using both surface electron and scanning probe microscopies. Imaging is done simultaneously on areas with and without Au particles and on samples spanning an order of magnitude in particle coverages. Based on this, we establish the equations of motion that can generally describe the Ga droplet dynamics, taking into account three general features: the affinity of Ga droplets to cover steps and rough structures on the surface, the evaporation-driven transition of the surface nanoscale morphology from rough to flat, and the enhanced evaporation due to Ga droplets and Au nanoparticles. Separately, these features can induce either self-propelled random motion or directional motion, but in combination, the self-propelled motion acts to increase the directional motion even if the directional force is 100 times weaker than the random force. We then find that the Au particles initiate a faster native oxide desorption and speed up the rough to flat surface transition in their vicinity. This changes the balance of forces on the Ga droplets near the Au particles, effectively deflecting the droplets from these areas. The model is experimentally verified for the present materials system, but due to its very general assumptions, it could also be relevant for the many other materials systems that display self-propelled random motion.

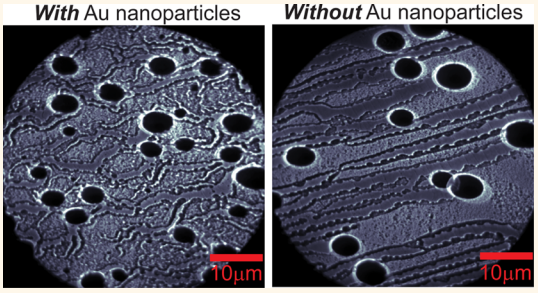

KEYWORDS: droplets · controlled self-propelled motion · III–V semiconductor · SPELEEM · SPM

The complex nature of droplet dynamics on surfaces has been an area of fascination and interest since the 19th century, as it demonstrates the intricate interplay between atomic, molecular, and nanoscale structures and forces to steer macroscopic dynamics.[1] In addition, droplet dynamics are central for a broad range of applications such as inkjet printing, self-cleaning surfaces, and lab-on-a-chip systems.[2−7] In the case of III–V semiconductors, droplets consisting of the group III material appear naturally due to noncongruent evaporation of the group V element. This type of droplet is important for fabrication of semiconductor nanostructures and electronic devices.[8−15] Interestingly, it has been observed in several recent studies[16−21] that these droplets tend to move around on the surface in so-called self-propelled motion, leaving a highly ordered trail behind them. More generally, self-propelled motion is a result of compositional or chemical alteration of the surface beneath a droplet and has been observed for a wide range of materials systems, ranging from brass alloys, metals on silicon, and long-chain alkanes to III–V semiconductors.[16,22,23] It can be explained by a permanent structural change beneath the droplet (for example, formation of a surface alloy) due to the interaction between the droplet material and the substrate. This leads to a change in local surface free energies that makes it favorable for the droplet to move away from its original position.[22−25] As will be discussed more in detail below, this often leads to a random motion with the only restriction that the

* Address correspondence to anders.mikkelsen@sljus.lu.se.

Received for review February 24, 2015 and accepted April 16, 2015.

Published online April 16, 2015
10.1021/acsnano.5b01228

droplet avoids its own trail—so-called non-overlapping random motion.[22−24] To complicate matters, it has been found that basic morphological surface features such as atomic steps and kinks can also play an important role in droplet motion.[17,26,27] The lower coordination number of the atoms at the steps can make it energetically favorable for the droplet to attach to the step. This can then lead to droplet motion along the steps[26,27] or in some cases even perpendicular to the step direction.[14] Usually, models have been considered where a single droplet propulsion mechanism dominates; however, in the present case, we show that even when several mechanisms have to be considered, robust and predictable motion can be observed.

One challenge of self-propelled droplets is the lack of control as motion is governed by features that are not easily designed, such as thermal fluctuations, detailed surface morphology, or crystallographic directions. A proven way to create controlled micro- and nanometer scale metal patterns is by e-beam or optical lithography, making the influence of metal nanostructures on group III droplet dynamics a rather interesting question. Au nanoscale structures, in particular, are fabricated on III−V surfaces for use as both electrical contacts and templates for controlled nanowire growth.[28] When a Au pattern is heated, it will turn into nanometer-sized Au particles from which nanowires can be grown. This situation is well-known for the present materials system of GaP, where it has, for example, been used to make ordered arrays of nanowires for fundamental growth studies and development of novel nanostructures and direct band gap GaP.[29−32] The III−V substrate of GaP(111)B in our study is the standard substrate for nanowire growth and has been shown to have rich Ga droplet dynamics, although its surface structures are fairly simple and well-defined.[33,34] To study the effect of Au nanoparticles, we use size-selected aerosol particles.[35] This type of Au particle has been used for numerous nanowire growth studies and has the advantage that they ensure an extremely clean and well-defined materials environment, including the absence of unwanted organic residues that are sometimes found for other types of Au particle fabrication methods.[36,37]

In the present paper, we find that Au nanoparticles influence the structure of the surrounding substrate locally in a way that can be used to influence and steer the motion of micron-sized Ga droplets. We establish a model that can generally describe the Ga droplet motion, taking into account all (experimentally measured) structural features on the surface as well as the presence of the Au particles. Finally, we present additional measurements with lower densities of Au particles that indicate how control of the Ga droplet motion can be achieved directly by the Au nanoparticles and which can be predicted by our theoretical model.

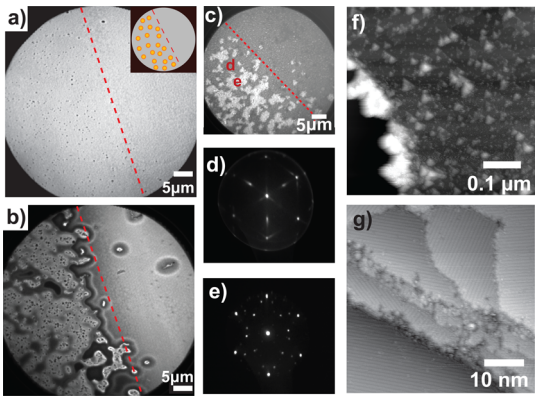

Figure 1. Description of the overall features of the Au nanoparticle−GaP(111)B surface system. (a) Mirror electron microscopy (MEM) image of the surface prior to annealing. Half the sample is covered with 50 nm diameter gold nanoparticles (left), and the other half (right) has no Au particles, as illustrated in the schematic drawing (inset). Au particles can be seen as black dots on the left half (MEM, −0.3 eV). (b) MEM image taken from a movie recorded during oxide desorption at ∼650 °C (see M1 in Supporting Information) of the same sample area as imaged in (a). (c) LEEM image recorded after the desorption of the native oxide (but prior to Ga droplet formation). Bottom left area contains Au particles, and the top right region contains no Au particles. (d,e) μLEED patterns recorded from the dark and bright regions, respectively in (c). (f) AFM image of the randomly dispersed pyramid structures found outside the droplet trails; there are several thousand per square micrometer. At this stage of the process, annealing has led to a significant decrease in island size compared to the point right after oxide removal. (g) STM image of several domains of the "Hattori" structure, which is found in the droplet trail and between the nanopyramids.

RESULTS AND DISCUSSION

To simultaneously study Ga droplet dynamics both with and without Au nanoparticles (50 nm diameter), half of the GaP(111)B surface was covered with Au particles, while the other half was left without. The well-defined boundary between the two parts of the sample can then be observed using synchrotron-based *in situ* spectroscopic photoemission and low-energy electron microscopy (SPELEEM), as seen in Figure 1a. The various modes of this surface electron microscope are described in the Methods section. By increasing the temperature of the sample to ∼650 °C, while imaging with the microscope, we can directly observe desorption of the native oxide as a contrast change initiated at the Au particles and then sweeping across the surface (see Figure 1b and movie M1 found in the Supporting Information). The removal of the surface oxide is confirmed both by O 1s X-ray core-level photoemission measurements and the appearance of a low-energy electron diffraction (LEED) pattern everywhere on the surface, as observed in the microscope.

Low-energy electron microscopy (LEEM) images of regions with/without Au particles after oxide desorption, as seen in Figure 1c, show the appearance of bright areas in Au-particle-covered regions. The difference in contrast is due to different diffraction conditions

induced by changes in the surface structure around the Au particles. Each of these bright areas can be directly correlated with the position of Au nanoparticles as imaged in the same region prior to annealing. By recording μLEED patterns from the bright and dark regions (Figure 1d,e) and comparing them to previous work,[17] we can conclude that the atomic scale structures are similar to what has been observed previously on clean GaP(111) but with different ratios between two different structural features (which we now describe). On the clean surface, nanopyramid structures are observed just after oxide removal, resulting in a very rough surface. The nanopyramid structures have base lengths and heights ranging from a few nanometers to tens of nanometers and are homogeneously distributed across the surface. As discussed in more detail elsewhere,[34] the pyramids consist of GaP and have {110} and smaller {114} facets and many undercoordinated corner and side sites. When annealing between 700 and 750 °C, these pyramids gradually evaporate while keeping the same shape and facets. As the pyramids disappear, they expose a flat six-fold domain structure, as first determined by Hattori *et al.*[33] (which we hence will call the Hattori structure). Beyond the evaporation of the pyramids and the appearance of the Hattori structure, no additional ordered structures or structural transformations are observed on the surface if the annealing is continued. As shown by the similarities of the μLEED patterns and by atomic force and scanning tunneling microscopy (AFM/STM) (as seen in Figure 1), the same two types of structure as just described are also found with the Au particles present. The brighter appearance on the LEEM images of the areas around the Au particles can be attributed to the nanopyramids having evaporated to a larger extent and thus exposing a larger areal fraction of the Hattori structure. This is established by measurements of μLEED patterns, which show that bright areas have a strong contribution from the diffraction spots of the Hattori structure as compared to the areas with no Au particles, which mostly show diffraction spots associated with the nanopyramid structures at this point of annealing. We therefore conclude that the transition from the rough nanopyramids to the flat (smooth) Hattori structure occurs much faster in the region around the Au particles as compared to the clean surface. This behavior cannot exclusively be explained by the faster initial desorption of the surface oxide around the Au particles. The Au particles must also induce faster evaporation of the pyramid structures. If this was not the case, the time delay between the evaporation of nanopyramids from areas without and with Au particles would be equal to the time delay between the oxide removal from the two areas. Instead, we observe that it takes much longer for the areas without Au particles to reach a situation where the pyramids have evaporated, which means that Au particles must also speed up the evaporation of the pyramid structures. Therefore, we conclude that the presence of the Au particles results in a faster desorption of both the native surface oxide and the nanopyramidal structures found after deoxidation. This dramatic influence of the Au particles during annealing of the substrate (as seen is this study) seems not to have been realized before, although it could certainly also be relevant for modeling, for example, nanowire growth.[32] The possible influence of Au nanoclusters on catalytic processes and the substrate on which they are adsorbed have been documented in recent years.[38−40] In addition, for GaAs nanowire growth, it has been shown that the Au seed particle can promote various group III and group V dissociation processes.[41] While the faster oxide desorption and the faster nanopyramid evaporation must be seen as two separate effects, both could be explained by the Au particles affecting the electronic properties of the surface or enhancing desorption of As species leading to different energetics for deoxidation and evaporation.

Annealing the GaP surface between 700 and 750 °C after this initial oxide desorption leads to the formation of clearly distinguishable Ga droplets appearing as dark spots in the LEEM image of Figure 2a. The formation and movement of the droplets can now be followed live in our surface microscope as seen in Figure 2 and in movie M2 (see Supporting Information). As the droplets move across the surface, they grow in size up to several microns and leave behind them clearly distinguishable trails. Tracking the droplet motion over time, as seen in Figure 2b, we observe that the droplets nucleate in the region with Au particles, moving slowly and in irregular patterns in this region. Still, they are, on average, moving from left to right in the image, which is the direction perpendicular to the average surface step direction. As soon as they cross over into the part of the sample with no Au particles, they start to move faster and unidirectional, following the average direction also of the Ga droplets in the Au-covered part.

The micron to atomic scale surface structures with and without Au particles at different stages of the Ga droplet movement can now be determined: We focus on the point when Ga droplets have created trails across the surface without completely removing the original rough areas, as all relevant structural features are found at once. We find using μLEED that only the atomically flat six-fold domain Hattori structure is observed inside the droplet trails, while outside the droplet trails, diffraction spots originating from both the nanopyramid structures and the Hattori structure are observed. To establish the structural development underneath the droplets, we note that after the droplets have passed an area with pyramids only the Hattori structure is observed in the trail, with no or extremely few pyramids left. This structural development

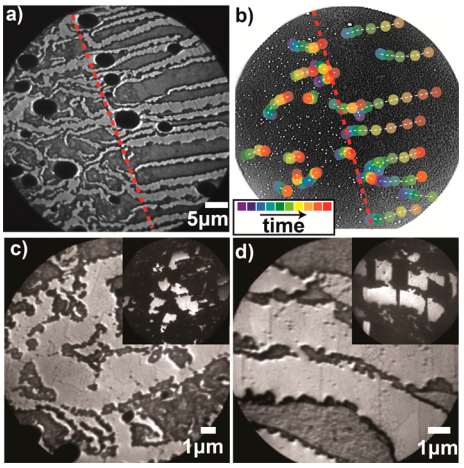

Figure 2. (a) LEEM image (2.2 eV) of Ga droplets and their trails on the boundary between the surface area with (left) and without (right) Au particles. The image is recorded of the same area as in Figure 1a. The Ga droplets appear as dark spots in the image. (b) Droplet motion has been traced out in every tenth frame of a movie (the time between frames is 1.6 s) recorded in MEM mode (−0.1 eV) during annealing at around 750 °C. The droplet traces have then been overlaid on a MEM image recorded before droplets were formed, in which the positions of the Au particles are seen. The image is the same as in Figure 1a, but its colors have been inverted for clarity. (c) LEEM image from the surface area with Au particles. Inset: Dark-field LEEM (DF-LEEM) image from the same area. Domains with straight edges are filling out the terraces separated by smooth steps perpendicular to the trail direction. (d) LEEM image from the surface area without Au particles. Inset: DF-LEEM image from the same area. The domains are rough and disordered although clearly larger than in the areas outside the droplet trails. In the areas between the trails, clear differences are also observed. For both (c) and (d), the μLEED patterns for the dark areas (outside the trails) indicate the presence of nanopyramids, and bright areas (inside the trails) have no nanopyramids and thus only the Hattori structure. LEEM images in (c) and (d) are recorded at 10 eV.

is identical to what can be observed also in areas where no droplets have passed, but after much longer annealing times (at the same temperatures). This is physically reasonable because the increased Ga content near and under the liquid Ga droplet can lead to changes in the melting energies on the surface. Increased melting rates of GaAs in the presence of liquid Ga have indeed been observed previously,[42,43] and the mechanism is still used today for pit etching.[44] So from our measurements, we propose that the pyramid sublimation process underneath the droplet is similar to the one on the free surface, just that it proceeds much faster.

There is no difference between the LEED patterns (and LEED spot intensities as a function of electron energy) from the regions with/without Au particles, which indicates that the atomic scale structures are the same. While this does not rule out small amounts of Au diffusing on the surface, it shows that no new atomic scale reconstructions (involving the Au) are introduced. Differences are instead found on the tens of nanometers up to micrometer scales. In the areas without Au particles, the droplet trails contain large single domains of the Hattori structure, separated by steps or step bunches perpendicular to the droplet trail direction (Figure 2d). In the Au-covered regions, there are also large single domains of the Hattori structure in the droplet trails and no remaining nanopyramids. However, the domain structure and the steps separating them are irregular and not necessarily perpendicular to the droplet trail direction (Figure 2c).

We can now propose an equation of motion for the Ga droplets explaining the observed behavior by taking into account the surface structure and morphology. Taking a step-by-step approach, we start by modeling the influence of the evaporation of the nanopyramids discussed above, explaining how they can lead to Ga droplets to perform non-overlapping self-propelled random motion.[16,22−25] For our model, two observations are most relevant: First, underneath the Ga droplets, the nanopyramids sublimate much more rapidly than from the free surface, leading to an alteration of the area beneath the droplet compared to the surroundings (a prerequisite for self-propelled droplet motion). Second, it has often been found that it is more favorable for a free species (such as Ga) to adsorb at under-coordinated defect sites on a surface.[45] It is therefore reasonable to assume that the rough nanopyramid-covered surface must be more energetically favorable for the droplets to occupy than the flat surface areas as the rough pyramids have many more under-coordinated sites. This will induce a driving force for droplet motion away from their trail, toward the regions still covered with pyramids. As this is an important assumption, we validate it experimentally by observing the behavior of less mobile droplets found by lowering the annealing temperature (Figure 3 and movie M3). Here we find that the droplets are pinned to rougher areas of the surface such as steps or step bunches, which is again reasonable if Ga adsorption on the lower coordinated sites is favored, and as a result, considerable energy will be required for the droplet to move out of this local energy minimum. As seen in the image series in Figure 3, the droplet stretches out 0.5 μm along the red line over a period of 24 s. After this period, the droplet retracts in less than one frame (1.6 s) and returns to its original position. After it has retracted, we can see that the area it left behind is now free from the nanopyramidal structures and only has the flat Hattori structure left. This illustrates how the droplet is attracted to the rough nanopyramid-covered areas, in this case resulting in an energetically less favorable elongation of the droplet (perturbing it from its circular equilibrium shape). This extension, however, only lasts until the nanopyramids are gone and the droplets then return to their original shape. We have observed the pinning of the droplets at lower temperatures both with and without Au particles and must thus conclude that it is independent of the presence of the Au particles.

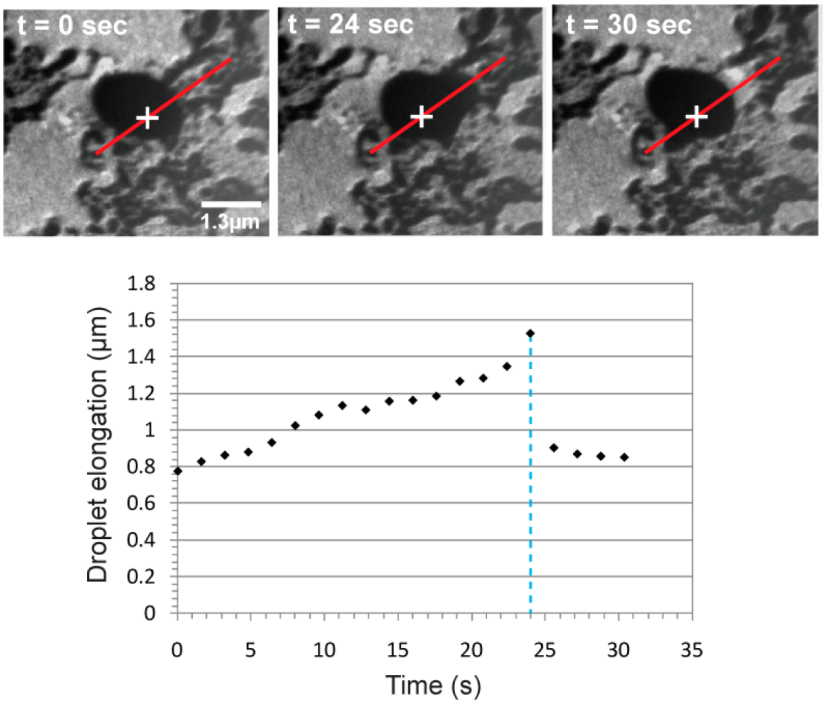

Figure 3. Three frames from a LEEM movie (15.9 eV, $T \sim 660$ °C). The droplet stretches toward a pyramid-covered area on the surface, dissolves the pyramids in 24 s, and returns to its original position (blue dashed line in the diagram). In the diagram, the elongation of the droplet in the direction of the red line has been measured relative to the point marked by the white cross.

Now establishing an equation for the motion of droplets due to the presence of the pyramids, we start with the (isotropic) case of an equal distribution of pyramids over the whole surface. Since the droplet "sees" an equal distribution of pyramids in all directions, even though it is energetically favorable for the droplet to move into these areas, the equal force attraction from all directions should lead to no net force and thus, in principle, no motion. However, motion will still occur because random thermal fluctuations displace the droplet, exposing the area beneath the droplet (in some direction), leading to unbalanced forces, and motion starts in the direction opposite to the exposed area. As the smooth areas left behind by the droplet are energetically less favorable, the motion will ensue with a preference against the droplet crossing its own trail or moving backward.[22,24,25] This is illustrated in Figure 4a. Such droplet motion can be described in an equation of motion as in the work by de Gennes[24] and later by Sumino *et al.*[25]

$$m\vec{a} = -\eta\vec{v} + \varepsilon(\vec{v})\frac{\vec{v}}{|\vec{v}|} + \vec{\zeta}(t) \qquad (1)$$

Here, the first term $(-\eta\vec{v})$ represents the drag due to viscosity, which acts linearly with the constant η in the opposite direction of the droplet motion $\vec{v}$. The second term $(\varepsilon(\vec{v})(\vec{v}/|\vec{v}|))$ is the driving force due to the droplet gradually changing the surface underneath itself (in the present case, by evaporation of the pyramids). ε depends on the specific type of reaction underneath the droplet. The third term $(\vec{\zeta}(t))$ represents random thermal fluctuations. This is a general model which can represent a number of different reaction types (and thus materials systems) by changing the function $\varepsilon(\vec{v})$.[24] For very fast reactions, the reaction has fully occurred before any further movement of the droplet takes place, yielding a constant value of ε. For slow reactions, the longer a droplet stays in one position (thus the slower it is), the farther the reaction has come and thus the stronger the force due to the structural changes induced by the reaction, a value of ε proportional to $(1/|\vec{v}|)$. Indeed, these two types of dependences have been observed for different material systems.[22−25] As we do not observe pyramids in the droplet trail, this indicates a very fast removal rate of pyramids in the trail compared to the speed of the droplet, which would, in turn, indicate that the force reaction rate in our case should be $\varepsilon(\vec{v}) = \text{const}$.

We can then add a term to eq 1 representing the influence of the Au nanosized particles. Thus, we consider the situation depicted in Figure 4b: As discussed above, the Au particles lead to a faster sublimation of the pyramid structures in a radius R_{Au} around the Au particles. Therefore, it is less energetically favorable for the droplet to move toward an area close to the Au particle than to an area where the pyramid structures are intact. In the limiting case of the pyramids having completely disappeared around the Au particle, this corresponds to the Ga droplets encountering areas that have previously been occupied by themselves. The situation can be described

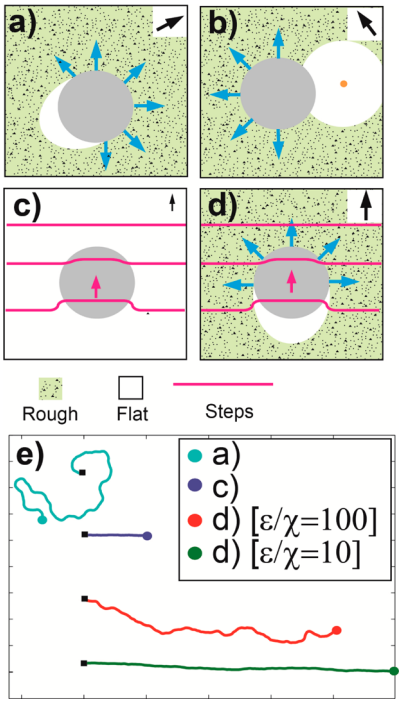

Figure 4. (a) Surface with a homogeneous distribution of pyramids (homogeneous roughness). Once a trail has been started by random fluctuations, the droplet will be drawn away from the trail regions. Forces on the droplet are indicated by blue arrows; the black arrow in the inset indicates the direction of motion. (b) When the surface roughness is not homogeneous (nanopyramid sublimation induced by the Au particles leads to this inhomogeneity), there will be an additional force on the droplet that affects its direction of motion. The droplet will feel a force toward the areas with a higher density of pyramids. (c) It is energetically favorable for the droplet to sit on a step edge. Sublimation of steps is enhanced under the droplet which is dragged along with the steps. It costs energy to distort a step, and eventually, the droplet will let go of the step and move to the next one. The force direction from the step-induced mechanism is indicated by the purple arrow. (d) Force due to the steps will move the droplets in a particular direction, which will then be enforced by the non-overlapping random force due to the pyramids. (e) Different simulated droplet path with different ratios between forces of eqs 1 and 3. Top simulation (light blue) is with only the self-avoiding random force illustrated in (a): The second (dark blue) is with only the step directional force (at the same magnitude as for the curves below) as illustrated in (c). The lowest two are with different ratios between the self-avoiding random forces and the step-directed force resulting in controlled motion (the step-directed force always being smaller than the random force). Steps are assumed to be vertically aligned. ζ and η have the same values for all cases with $\zeta/\varepsilon = 0.02$ and $\eta/\varepsilon = 0.2$.

(see Supporting Information for more details) by a force on the Ga droplet directed away from the Au particle:

$$\vec{F}_{Au-Ga} = \varepsilon_{Au} \frac{\vec{r}_{Au-Ga}}{|\vec{r}_{Au-Ga}|} \sqrt{\Delta r / R_{Ga}}$$

$$\text{for } \Delta r > 0; \Delta r = (R_{Ga} + R_{Au}) - |\vec{r}_{Au-Ga}| \quad (2)$$

where $\vec{r}_{Au-Ga}$ is the vector pointing from the Au particle to the Ga droplet center, R_{Ga} and R_{Au} are the radii of the areas affected by the Ga droplet and Au particles, respectively, and ε_{Au} is a constant which will be smaller than or equal to the ε found in the force generated by the sublimation of pyramids by the Ga droplet.

We finally need to expand this model to add the influence of the steps and step sublimation, as indicated in Figure 4c. From extensive SPELEEM and STM measurements on the clean surface,[17] we found unidirectional droplet motion perpendicular to and up the surface steps. Similar behavior has later been found for Au droplets on Si.[46] The mechanism behind this motion can be understood based upon two properties of the materials system briefly developed here: First, as discussed above, there is a strong affinity for the droplets toward covering rough surface areas (on an atomic level, this can be understood as the energy gained by Ga adsorption increases as the coordination number of the site on the GaP surface decreases[17]). Aside from the pyramids, the other sources of undercoordinated sites are surface steps and kinks, which will lead the droplet to cover as many steps and kinks as possible. This alone would result in the droplets being pinned to the surface steps, a behavior observed previously for Pt−Si particles on Si.[27] Thus, a second property of the system is needed to explain the observed droplet motion—step sublimation that occurs (at least) beneath the droplet. Considering the case of parallel uniform steps, sublimation of the steps underneath the droplets will result in the position of the steps moving forward perpendicular to the step, as illustrated in Figure 4c. As we established that the droplet minimizes its energy by covering the steps, it will be dragged along with the steps. If the droplet only covers one step, motion will quickly stop as it costs energy to distort a step.[47] However, if the droplet radius $R_{droplet} > R_{step}$ (the distance between the steps), the droplet will meet new steps as it progresses forward and will minimize its total energy by covering also the new steps and thus releasing the old distorted ones (as further distortions are too energetically costly), which will then stop moving. This can effectively be represented as a force pulling in the direction perpendicular to and up the surface steps.[17] Thus, we define a constant force perpendicular to the surface steps (described in Figure 4c):

$$\vec{F} = \chi \frac{\vec{r}_0}{|\vec{r}|} \quad (3)$$

Here, we let the force take the simplest linear form and define it to be a constant in the direction r_0, which is perpendicular to the step direction; χ represents the strength of the force.

Armed with eqs 1, 2, and 3, we are now capable of simulating the behavior of the full sample system, with nanopyramids, steps, and Au nanoparticles. Separating out the different effects first in our modeling, we start

with the situation of only the pyramid structures (Figure 4a). We can simulate paths of droplet motion, solving the differential eq 1. This leads to the self-avoiding random motion path exemplified in Figure 4e. The motion as predicted by eq 1 is a quite general phenomenon and has (as noted above) been observed for very different materials systems.[22−25] In the present case, we have verified experimentally (as discussed above) that the ingredients necessary for non-overlapping random motion are present, and without other effects, this would be the motion pattern we would expect. As we now discuss, the reason why this is not observed on this GaP surface is due to the influence of the steps. If we first take the force due to the pyramids out of our model (set $\varepsilon = 0$), but add the effect of the steps (eq 3) and again numerically solve this differential equation, we see the effect of the steps separately. The obtained result in Figure 4e shows that motion in a straight line perpendicular to the step direction will occur, as observed in our previous experiments.[17] This is thus in agreement with our experimentally observed behavior on the free surface. However, things get really interesting when we now add eqs 1 and 3 and simulate the combined effect on the droplet motion. As seen in Figure 4e, even with the step-induced force being 100 times smaller than the force due to pyramid sublimation ($\varepsilon/\chi = 100$), the droplet will now move in the direction of the force due to the step sublimation. Importantly, if we now compute a number of trajectories for the system of a droplet influenced by both forces (with the force due to the steps being 10 times smaller than the force due to sublimation of the pyramids), the droplet will travel 10 times longer (over the same time period) compared to a droplet only influenced by the directional step force. In fact, we can make the general statement that the self-propelled motion described in eq 1 will act to radically increase the effect of any other, even 100 times smaller, force that pushes the droplet in a specific direction. Usually, a self-avoiding random motion mechanism would not be perceived as a very useful propulsion concept for droplets as it is highly uncontrolled, and one would thus tend to suppress it unless the droplets are forced to move along one-dimensional guides. Here it is found that any small directional force induced by steps (as in the present case) would instead be strongly enhanced by the self-avoiding random motion mechanism. A simplified way to understand how this somewhat surprising effect is, in fact, reasonable is to come back to the well-established basics of self-avoiding random motion. From Figure 4a, one realizes that while it is unfavorable for the droplet to move backward it is equally favorable to move to any of the two sides. Thus, depending on random thermal fluctuations, it can move forward and to either the left or right, which will induce the randomness of the motion. However, adding a small directional force will shift this balance, and there will now be a preference toward moving in the direction of this extra force. If the contribution due to this force is larger than the thermally induced fluctuations, the droplet will then move in the direction of this force as the random fluctuations will no longer be a deciding factor for the movement direction. In the case of the clean surface, the difference that self-avoiding random motion will make is to enhance the speed of the droplet motion that is then steered by the step directional force. This also explains why it can be difficult to directly observe self-avoiding random motion on this surface. The two forces inherently act together, and as they in the present case both depend on surface roughness, they will have comparable magnitudes. However, as we discuss now, by introducing the Au particles to change the local surface structure and thus the balance of forces locally in the system, we can see the interplay between the two effects. Adding also the influence of the Au particles in the modeling, we find for high densities of Au particles (as in Figure 2) a substantial randomization of the movement the droplets as they try to avoid the areas with Au particles. This combined with the Au particles generally lowering the amount of nanopyramids at these high densities leads to the movement and randomized trails described for the Au-particle-covered regions in Figures 1 and 2.

At this point, it is worth considering if other mechanisms could explain the droplet behavior. Our measurements clearly show that the change of droplet behavior is locally connected to the Au particles, but an alternative explanation would be that the Au atoms would somehow remove the influence of the steps, for example, by adsorption on the step edges or by incorporating in the Ga droplet. From the situation as shown in Figure 1 of a dense Au-nanoparticle-covered region, it might be difficult to clearly distinguish these two scenarios. However, for a less dense Au coverage, it should be possible to observe a difference. Our model predicts that Ga droplets will avoid the regions around the Au particle, while the removal of the influence of the steps would simply make the droplets continue their motion in a new (random) direction. This is a rather interesting issue as our model would indicate that the Au particles can more readily be used to steer the motion of the Ga droplets. We have made samples with a lower density of Au particles ($0.1/\mu m^2$) and imaged them again with surface electron microscopy. At these lower Au particle densities, we are capable of identifying areas affected by individual Au particles and observe their influence on individual droplet trails, which can be compared to simulations by our model, as seen in Figure 5. Here we have imaged the position of the Au particles prior to annealing and the trails formed by Ga droplets during annealing. The two images are then added on top of each other with the

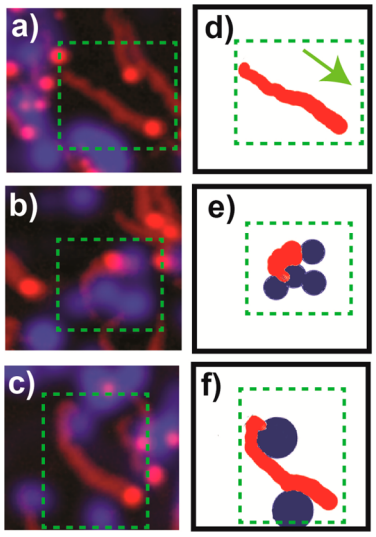

Figure 5. (a–c) We have placed two colored images on top of each other in order to investigate if the Ga droplets avoid the areas around Au particles. The blue spots represent the estimated area around each Au particle found on the surface before annealing as found using UV-PEEM. A UV-PEEM image of the droplets and their trails formed after annealing was colored red and overlaid on the blue image. (d–f) To the right of each of the experimentally obtained images, we show theoretically simulated Ga droplet trails (in red), with pyramids having been sublimated in the blue areas. In this model, we included the increasing size of the Ga droplet as estimated from the experimental data. The green arrow indicates the direction perpendicular to the surface steps in both the model and the experiment.

(blue) area affected by the Au particles (as estimated from Au nanoparticle position combined with the observed extent of their morphology influence) combined with the (red) Ga droplet trails. The direction of the steps on the surface is also known and is indicated by the green arrow. Three examples of Au particle positions were chosen to reflect three standard situations: no Au particles blocking the path of the Ga droplet, Au particles completely blocking the Ga droplet path, and Au particles close to the path of the droplet (deflection of the Ga droplet). The equal size of the Ga droplet in all three cases indicates that they have traveled for an equal amount of time. The trails of these three standard situations for motion control (free movement, stopping, and deflection) observed in Figure 5 can now be directly compared to pathways simulated using combined forces of eqs 1, 2, and 3 and placing Au particles affecting circular areas as found experimentally (indicated in Figure 5d–f in blue). We have used values for the forces that can replicate the motion on the Au-free part of the surface. As can be seen, the model will replicate the standard behaviors well. This shows that our model is capable of describing the system of GaP(111) and Au-nanoparticle-induced sublimation. From observing many instances of blocking and deflection, we generally find that the Ga droplets move away from the Au-particle-affected regions instead of continuing in random directions as would be the case for other explanations of the influence of the Au particle. Interestingly, our results also indicate that, while steps can be used to control the droplets, the presence of Au particles could be used to bend and distort the droplet trajectories. This can be used for steering a droplet on the surface by placing the Au particles in specific positions as can be done with lithographic methods.

CONCLUSIONS

We have studied the effect of Au nanoparticles on the self-propelled motion of Ga droplets on the GaP(111)B surface. We find that the Au nanoparticles locally affect the dynamics of the Ga droplets by modifying the surface structure in their surroundings, thereby changing the balance of forces on the Ga droplets. The Ga droplets tend to avoid the areas affected by the Au particles, opening a new route for controlling their motion. We put up a set of equations of the different forces affecting the complex system of Ga droplets, III–V surface nanostructures, and Au nanoparticles and show how this unified model can be used to robustly predict the droplet motion even when several forces are at play. We find that several motion mechanisms in conjunction can lead to new behavior, which is not just a superposition of the individual ones. This can lead to new and quite useful enhanced directional motion. In our model, the understanding of how the morphology and atomic scale structure change the forces that control the Ga droplet motion can be used to model the effect of the Au nanoparticles, predicting the motion patterns of the Ga droplets and thus giving a tool for designing surfaces where droplets will move in specific ways. Since the forces included in our model are very general and can arise in many different systems, our insights and approach should be applicable to a wide variety of materials systems. Important III–V compounds and many other materials are conceivable, where self-propelled droplet motion occurs in combination with other forces and local chemical modifications.

METHODS

The GaP(111)B samples were cut from an epi-ready S-doped wafer (10^{17}–10^{18} cm^{-3}). Au nanoparticles of varying size and density, 50–100 nm in diameter and 0.1–1 particles/μm^2, were deposited by an aerosol deposition method described elsewhere.[35] LEED, LEEM, and MEM measurements were performed with an Elmitec LEEM III connected to the soft X-ray beamline 311 at the MAX-lab synchrotron in Lund, Sweden.[48] The different operational modes of the microscope are described in ref 49. Here, we give a very brief account. In MEM, the electrons are reflected before they hit the surface, giving a

contrast very sensitive for geometric features on the surface. However, due to field distortion, objects like droplets will appear distorted in size. In the LEEM mode, the electrons have high enough energy to penetrate the surface (usually from a few up to tens of electronvolts), and we then image the (elastically) backscattered electrons. The bright areas in the LEEM images indicate areas of high surface order (intense 0,0 diffraction spot). Using an aperture in the diffraction plane, electrons from specific diffraction spots can also be imaged. In this dark-field mode, bright areas will indicate regions that have the specific diffraction spot. μLEED patterns from an area down to 0.16 μm^2 could be recorded by inserting apertures in the SPELEEM. Ultraviolet photoemission electron microscopy (UV-PEEM) measurements were also done with the Elmitec SPELEEM as well as with an Focus IS-PEEM. In this imaging mode, Au particles, Ga droplets, and the trails left behind the Ga droplets can be seen. The in-vacuum STM measurements were performed with commercial Omicron VT STM XA, at a base pressure below 1×10^{-10} mbar. Electrochemically etched tungsten tips were used, and images were acquired in the constant current mode. AFM measurements in air were performed using a Digital Instruments Dimension 3100 AFM. Since the GaP only forms a few nanometer thick homogeneous oxide upon air exposure, the general morphology found in vacuum after annealing will be preserved. The simulated droplet paths shown in Figure 4 and Figure 5 are based on solving the differential eq 1 (with terms of eqs 2 and 3 added as described in the text) using a standard Runge−Kutta (ode45) solver in MATLab.[50]

Conflict of Interest: The authors declare no competing financial interest.

Acknowledgment. The authors want to thank the MAX IV laboratory staff for experimental support. This work was performed within the Nanometer Structure Consortium at Lund University (nmC@LU) and was supported by the Swedish Research Council (VR), the Swedish Foundation for Strategic Research (SSF), the Swedish energy agency, the Crafoord Foundation, the Knut and Alice Wallenberg Foundation, and the European Research Council under the European Union's Seventh Framework Programme Grant Agreement No. 259141.

Supporting Information Available: Description of movies M1−M3 and a calculation of forces on the droplet when rough nanopyramid-covered areas have evaporated due to the presence of the Au particles (eq 2 of the article). This material is available free of charge *via* the Internet at http://pubs.acs.org.

REFERENCES AND NOTES

1. Israelachvili, J. N. Intermolecular and Surface Forces. In *Surface and Intermolecular Forces*, 3rd ed.; Elsevier: Amsterdam, 2011; ISBN: 0123919274.
2. Lee, J.-L.; Kim, M.-S.; Kim, D.; Kim, Y.-M.; Moon, J.; Joo, S.-K. Fabrication and Characterization of Low Temperature Polycrystalline Silicon Thin Film Transistors by Ink-Jet Printed Nickel-Mediated Lateral Crystallization. *Appl. Phys. Lett.* **2009**, *94*, 122105.
3. Somaschini, C.; Bietti, S.; Koguchi, N.; Sanguinetti, S. Fabrication of Multiple Concentric Nanoring Structures. *Nano Lett.* **2009**, *9*, 3419.
4. Sinz, D. K. N.; Darhuber, A. A. Self-Propelling Surfactant Droplets in Chemically-Confined Microfluidics—Cargo Transport, Drop-Splitting and Trajectory Control. *Lab Chip* **2012**, *12*, 705.
5. Chu, K.-H.; Xiao, R.; Wang, E. N. Uni-directional Liquid Spreading on Asymmetric Nanostructured Surfaces. *Nat. Mater.* **2010**, *9*, 413.
6. Galliker, P.; Schneider, J.; Eghlidi, H.; Kress, S.; Sandoghdar, V.; Poulikakos, D. Direct Printing of Nanostructures by Electrostatic Autofocussing of Ink Nanodroplets. *Nat. Commun.* **2012**, *3*, 890.
7. Yao, L.; He, J. Recent Progress in Antireflection and Self-Cleaning Technology—From Surface Engineering to Functional Surfaces. *Prog. Mater. Sci.* **2014**, *61*, 94.
8. Wang, Z. M.; Liang, B. L.; Sablon, K. A.; Salamo, G. J. Nanoholes Fabricated by Self-Assembled Gallium Nanodrill on GaAs(100). *Appl. Phys. Lett.* **2007**, *90*, 113120.
9. Somaschini, C.; Bietti, S.; Trampert, A.; Jahn, U.; Hauswald, C.; Riechert, H.; Sanguinetti, S.; Geelhaar, L. Control over the Number Density and Diameter of GaAs Nanowires on Si(111) Mediated by Droplet Epitaxy. *Nano Lett.* **2013**, *13*, 3607.
10. Wu, J.; Hirono, Y.; Li, X.; Wang, Z. M.; Lee, J.; Benamara, M.; Luo, S.; Mazur, Y. I.; Kim, E. S.; Salamo, G. J. Self-Assembly of Multiple Stacked Nanorings by Vertically Correlated Droplet Epitaxy. *Adv. Funct. Mater.* **2013**, *24*, 530.
11. Li, X.; Wu, J.; Wang, Z. M.; Liang, B.; Lee, J.; Kim, E.-S.; Salamo, G. J. Origin of Nanohole Formation by Etching Based on Droplet Epitaxy. *Nanoscale* **2014**, *6*, 2675.
12. Cavigli, L.; Bietti, S.; Accanto, N.; Minari, S.; Abbarchi, M.; Isella, G.; Frigeri, C.; Vinattieri, A.; Gurioli, M.; Sanguinetti, S. High Temperature Single Photon Emitter Monolithically Integrated on Silicon. *Appl. Phys. Lett.* **2012**, *100*, 231112.
13. Huo, Y. H.; Witek, B. J.; Kumar, S.; Cardenas, J. R.; Zhang, J. X.; Akopian, N.; Singh, R.; Zallo, E.; Grifone, R.; Kriegner, D.; et al. A Light-Hole Exciton in a Quantum Dot. *Nat. Phys.* **2014**, *10*, 46.
14. Wu, J.; Shao, D.; Dorogan, V. G.; Li, A. Z.; Li, S.; DeCuir, E. A.; Manasreh, M. O.; Wang, Z. M.; Mazur, Y. I.; Salamo, G. J. Intersublevel Infrared Photodetector with Strain-Free GaAs Quantum Dot Pairs Grown by High-Temperature Droplet Epitaxy. *Nano Lett.* **2010**, *10*, 1512.
15. Wu, J.; Wang, Z. M.; Dorogan, V. G.; Li, S.; Zhou, Z.; Li, H.; Lee, J.; Kim, E. S.; Mazur, Y. I.; Salamo, G. J. Strain-Free Ring-Shaped Nanostructures by Droplet Epitaxy for Photovoltaic Application. *Appl. Phys. Lett.* **2012**, *101*, 043904.
16. Tersoff, J.; Jesson, D. E.; Tang, W. X. Running Droplets of Gallium from Evaporation of Gallium Arsenide. *Science* **2009**, *324*, 236.
17. Hilner, E.; Zakharov, A. A.; Schulte, K.; Kratzer, P.; Andersen, J. N.; Lundgren, E.; Mikkelsen, A. Ordering of the Nanoscale Step Morphology as a Mechanism for Droplet Self-Propulsion. *Nano Lett.* **2009**, *9*, 2710.
18. Xu, X.; Wu, J.; Wang, X.; Li, H.; Zhou, Z.; Wang, Z. M. Site-Controlled Fabrication of Ga Nanodroplets by Focused Ion Beam. *Appl. Phys. Lett.* **2014**, *104*, 133104.
19. Zheng, C. X.; Tang, W. X.; Jesson, D. E. Asymmetric Coalescence of Reactively Wetting Droplets. *Appl. Phys. Lett.* **2012**, *100*, 071903.
20. Mandl, B.; Stangl, J.; Hilner, E.; Zakharov, A. A.; Hillerich, K.; Dey, A. W.; Samuelson, L.; Bauer, G.; Deppert, K.; Mikkelsen, A. Growth Mechanism of Self-Catalyzed Group III−V Nanowires. *Nano Lett.* **2010**, *10*, 4443.
21. Kanjanachuchai, S.; Euaruksakul, C. Self-Running Ga Droplets on GaAs(111)A and (111)B Surfaces. *ACS Appl. Mater. Interfaces* **2013**, *5*, 7709.
22. Schmid, A. K.; Bartelt, N. C.; Hwang, R. Q. Alloying at Surfaces by the Migration of Reactive Two-Dimensional Islands. *Science* **2000**, *290*, 1561.
23. Lazar, P.; Riegler, H. Reversible Self-Propelled Droplet Movement: A New Driving Mechanism. *Phys. Rev. Lett.* **2005**, *95*, 136103.
24. de Gennes, P. G. The Dynamics of Reactive Wetting on Solid Surfaces. *Physica A* **1998**, *249*, 196.
25. Sumino, Y.; Magome, N.; Hamada, T.; Yoshikawa, K. Self-Running Droplet: Emergence of Regular Motion from Nonequilibrium Noise. *Phys. Rev. Lett.* **2005**, *94*, 068301.
26. Wu, J.; Wang, Z. M.; Li, A. Z.; Benamara, M.; Lee, J.; Koukourinkova, S. D.; Kim, E. S.; Salamo, G. Critical Size of Self-Propelled Motion of Droplets on GaAs (100) Surface. *J., Appl. Phys.* **2012**, *112*, 043523.
27. Sutter, P.; Bennett, P. A.; Flege, J. I.; Sutter, E. Steering Liquid Pt−Si Nanodroplets on Si(100) by Interactions with Surface Steps. *Phys. Rev. Lett.* **2007**, *99*, 125504.
28. Fan, H. J.; Werner, P.; Zacharias, M. Semiconductor Nanowires: From Self-Organization to Patterned Growth. *Small* **2006**, *2*, 700.
29. Borgström, M. T.; Immink, G.; Ketelaars, B.; Algra, R.; Bakkers, E. P. A. M. Synergetic Nanowire Growth. *Nat. Nanotechnol.* **2007**, *2*, 541.
30. Assali, S.; Zardo, I.; Plissard, S.; Kriegner, D.; Verheijen, M. A.; Bauer, G.; Meijerink, A.; Belabbes, A.; Bechstedt, F.;

Haverkort, J. E. M.; et al. Direct Band Gap Wurtzite Gallium Phosphide Nanowires. *Nano Lett.* **2013**, *13*, 1559.
31. Dick, K. A.; Deppert, K.; Larsson, M. W.; Mårtensson, T.; Seifert, W.; Wallenberg, L. R.; Samuelson, L. Synthesis of Branched 'Nanotrees' by Controlled Seeding of Multiple Branching Events. *Nat. Mater.* **2004**, *3*, 380.
32. Wacaser, B. A.; Dick, K. A.; Johansson, J.; Borgstrom, M. T.; Deppert, K.; Samuelson, L. Preferential Interface Nucleation: An Expansion of the VLS Growth Mechanism for Nanowires. *Adv. Mater.* **2009**, *21*, 153.
33. Hattori, K.; Ishihara, K.; Miyatake, Y.; Matsui, F.; Takeda, S.; Daimon, H.; Komori, F. Gap($\bar{1}\ \bar{1}\ \bar{1}$) Reconstructed Surface Studied with STM and LEED. *Surf. Sci.* **2003**, *525*, 57.
34. Hilner, E.; Zakharov, A. A.; Schulte, K.; Andersen, J. N.; Lundgren, E.; Mikkelsen, A. Faceting and Surface Reconstruction of the Gap(111)B Surface. *Surf. Interface Anal.* **2010**, *42*, 1524.
35. Magnusson, M. H.; Deppert, K.; Malm, J.-O.; Bovin, J.-O.; Samuelson, L. Size-Selected Gold Nanoparticles by Aerosol Technology. *Nanostruct. Mater.* **1999**, *12*, 45.
36. Mikkelsen, A.; Eriksson, J.; Lundgren, E.; Andersen, J. N.; Weissenreider, J.; Seifert, W. The Influence of Lysine on InP(001) Surface Ordering and Nanowire Growth. *Nanotechnology* **2005**, *16*, 2354.
37. Grigorescu, A. E.; Hagen, C. W. Resists for Sub-20-nm Electron Beam Lithography with a Focus on HSQ: State of the Art. *Nanotechnology* **2009**, *20*, 292001.
38. Wahlström, E.; Lopez, N.; Schaub, R.; Thostrup, P.; Rønnau, A.; Africh, C.; Lægsgaard, E.; Nørskov, J. K.; Besenbacher, F. Bonding of Gold Nanoclusters to Oxygen Vacancies on Rutile TiO_2(110). *Phys. Rev. Lett.* **2003**, *90*, 026101.
39. Zhang, J.; Sasaki, K.; Sutter, E.; Adzic, R. R. Stabilization of Platinum Oxygen-Reduction Electrocatalysts Using Gold Clusters. *Science* **2007**, *315*, 220.
40. Choudhary, T. V.; Goodman, D. W. Oxidation Catalysis by Supported Gold Nano-clusters. *Top. Catal.* **2002**, *21*, 25.
41. Kratzer, P.; Sakong, S.; Pankoke, V. Catalytic Role of Gold Nanoparticle in GaAs Nanowire Growth: A Density Functional Theory Study. *Nano Lett.* **2012**, *12*, 943.
42. Lou, C. Y.; Somorjai, G. A. Studies of the Vaporization Mechanism of Gallium Arsenide Single Crystals. *J. Chem. Phys.* **1971**, *55*, 4554.
43. Rusell, G. J.; Ip, H. K.; Haneman, D. J. Vacuum Thermal Decomposition of III−V Compound Surfaces. *Appl. Phys.* **1966**, *37*, 3328.
44. Li, S.; Wu, J.; Wang, Z.; Li, Z.; Su, Y.; Wu, Z.; Jiang, Y.; Salamo, G. J. Thermal Etching Process of Microscale Pits on the GaAs(001) Surface. *Phys. Status Solidi RRL* **2012**, *6*, 25.
45. Michely, T.; Krug, J. *Islands, Mounds and Atoms*, Surface Science Series 42; Springer: Berlin, 2004.
46. Curiotto, S.; Leroy, F.; Cheynis, F.; Müller, P. Self-Propelled Motion of Au−Si Droplets on Si(111) Mediated by Monoatomic Step Dissolution. *Surf. Sci.* **2015**, *632*, 1.
47. Bartelt, N. C.; Tromp, R. M.; Williams, E. D. Step Capillary Waves and Equilibrium Island Shapes on Si(001). *Phys. Rev. Lett.* **1994**, *73*, 1656.
48. Zakharov, A. A.; Mikkelsen, A.; Andersen, J. N. Recent Advances in Imaging of Properties and Growth of Low Dimensional Structures for Photonics and Electronics by XPEEM. *J. Electron Spectrosc. Relat. Phenom.* **2012**, *185*, 417.
49. Bauer, E. *Surface Microscopy with Low Energy Electrons*; Springer: Berlin, 2014.
50. Dormand, J. R.; Prince, P. J. A Family of Embedded Runge-Kutta Formulae. *J. Comp. Appl. Math.* **1980**, *6*, 19.